Chinese Physics B

PAPER

Any-polar resistive switching behavior in Ti-intercalated Pt/Ti/HfO_2/Ti/Pt device*

To cite this article: Jin-Long Jiao *et al* 2021 *Chinese Phys. B* **30** 118701

Any-polar resistive switching behavior in Ti-intercalated Pt/Ti/HfO_2/Ti/Pt device*

Jin-Long Jiao(焦金龙)[1], Qiu-Hong Gan(甘秋宏)[1], Shi Cheng (程实)[1], Ye Liao(廖晔)[1], Shao-Ying Ke(柯少颖)[2], Wei Huang(黄巍)[1,†], Jian-Yuan Wang(汪建元)[1], Cheng Li(李成)[1], and Song-Yan Chen(陈松岩)[1]

[1] *Department of Physics and Jiujiang Research Institute, Xiamen University, Xiamen* 361005, *China*
[2] *College of Physics and Information Engineering, Minnan Normal University, Zhangzhou* 363000, *China*

(Received 21 January 2021; revised manuscript received 16 March 2021; accepted manuscript online 30 March 2021)

The special any-polar resistive switching mode includes the coexistence and stable conversion between the unipolar and the bipolar resistive switching mode under the same compliance current. In the present work, the any-polar resistive switching mode is demonstrated when thin Ti intercalations are introduced into both sides of Pt/HfO_2/Pt RRAM device. The role of the Ti intercalations contributes to the fulfillment of the any-polar resistive switching working mechanism, which lies in the filament constructed by the oxygen vacancies and the effective storage of the oxygen ion at both sides of the electrode interface.

Keywords: filament, memory, resistive switching

PACS: 87.15.La, 79.60.Dp, 81.05.–t, 81.15.Gh **DOI:** 10.1088/1674-1056/abf34e

1. Introduction

Resistive random access memory (RRAM) devices offer significant application potential in future non-volatile data storage technology[1–4] due to their fast operation speed, high storage density, and process compatibility with today's silicon technology.[5–7] In previous research of RRAM, the resistive switching modes are generally classified as unipolar resistive switching (URS) mode and bipolar resistive switching (BRS)[8] mode. If the URS can symmetrically occur at both positive and negative voltages, it is also referred to as non-polar resistive switching mode.[9,10] In recent years, coexistence of URS and BRS was also studied.[11–17] According to our previous study on Pt/LATP/Pt devices, the stable conversion between the unipolar mode and the bipolar mode is named any-polar resistive switching mode.[18] The crystalline channel structure of the LATP ($Li_{1-x}Al_xTi_{2-x}(PO_4)_3$)[19–21] benefits the easy movement and effective storage of the oxygen ion when used as a resistive switching layer, and thus contributing to the any-polar resistive switching mode.

Titanium (Ti), as a metal with high affinity with oxygen, is naturally regarded as an ideal oxygen storage material. Using Ti as an electrode or additional interfacial layer to improve the performance of RRAM device has been extensively studied.[22,23] For the widely studied HfO_2 RRAM, with a thin Ti layer serving as a reactive buffer layer, the TiN/Ti/HfO_2/TiN device demonstrated excellent memory performance and satisfactory switching endurance over 10^6 cycles.[23]

In this work, the effect of Ti intercalation on the conventional HfO_2 resistive switching device is restudied. The Ti intercalation can be at one side of the HfO_2 film, or be at each side of the HfO_2 film. With various device structures, different resistive switching modes are found. When the Ti intercalation layers are inserted at both sides of the HfO_2 film, the resulting Pt/Ti/HfO_2/Ti/Pt device shows the stable any-polar resistive switching behavior. This phenomenon gives a new insight into the fundamental working mechanism of the any-polar resistive switching mode.

2. Results and discussion

To fabricate HfO_2 RRAMs, the Pt-substrate is used as a bottom electrode. The Pt-substrate contains a structure of Pt(100 nm)/Ti(50 nm)/Si(100), which is prepared by successive direct current (DC) magnetron sputtering of Ti and Pt on a Si(100) substrate. The resistive HfO_2 layer is then grown by atomic layer deposition (ALD) at 275 °C with using tetrakis (sthylmethylamido) hafnium (TEMAH) and H_2O as precursors. A 5-nm-thick Ti layer is sputtered at the front side and/or at the back side of the HfO_2 film as an intercalation layer. The Pt top electrodes with a diameter of 800 μm are sputtered through a mechanical mask.

As shown in Fig. 1(a), three types of resistive memory devices are prepared in the present investigation, which are Pt/HfO_2(10 nm)/Pt, Pt/HfO_2(10 nm)/Ti(5 nm)/Pt, and Pt/Ti(5 nm)/HfO_2(10 nm)/Ti(5 nm)/Pt. For basic DC *I*–*V* measurements, an external bias is applied to the top Pt elec-

*Project supported by the National Natural Science Foundation of China (Grant Nos. 62004087, 61474081, and 61534005), the Natural Science Foundation of Fujian Province, China (Grant No. 2020J01815), the Natural Science Foundation of Zhangzhou, China (Grant No. ZZ2020J32), and the Natural Science Foundation of Jiangxi Province, China (Grant No. 20192ACBL20048).

†Corresponding author. E-mail: weihuang@xmu.edu.cn

trode, and the bottom Pt electrode is grounded by a Keithley 4200 semiconductor parameter analyzer. All measurements are performed respectively at room temperature, in ambient condition, and in a dark chamber. Transmission electron microscope (TEM) is used to image the cross-section of the Pt/Ti/HfO_2/Ti/Pt-substrate device as shown in Fig. 1(b). The TEM samples are prepared by applying the *in situ* focused ion beam lift-out technique to a dual beam, for focused ion beam/scanning electron microscopy (FEI Company, UK).

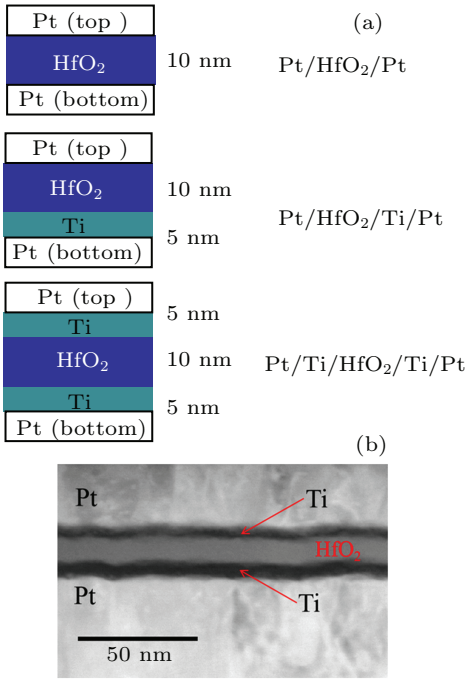

Fig. 1. (a) Schematic diagram of RRAM devices with Ti intercalation layers, and (b) cross-section of the Pt/Ti/HfO_2/Ti/Pt device.

The simplest RRAM can be finished by a simple sandwich structure of metal/oxide/metal such as Pt/HfO_2/Pt. The Pt/HfO_2/Pt RRAM works in URS switching mode. However, the Pt/HfO_2/Pt RRAM suffers poor endurance property. After limited switching cycles, the device tends to be break down.[24] Figure 2(a) shows the current–voltage (I–V) switching property of our Pt/HfO_2/Pt RRAM. The initial high resistance state (HRS) of the as-fabricated device is about 10^{10} Ω. After electroforming, the RESET voltage is around 0.5 V, and the SET voltages are in a range between 1.5 V and 4.3 V for the following cycles. The on-off ratio at a read voltage of 0.2 V is generally larger than 10^3. But after 10 cycles, the device fails, ending up with final permanent low resistance state (LRS). The limited switching cycles lie in the oxygen ions migrating towards and escaping from the anode electrode during the switching. This was also confirmed by the observation of gas bubbles at the anode in early studies.[2]

To improve the switching property of the Pt/HfO_2/Pt RRAM, titanium electrode or titanium intercalation layer is introduced. Considering that the oxygen ion is the moving species under switching operations and with the titanium layer acting as the oxygen reservoir, the duration property of the HfO_2 RRAM device is prominently improved.[23] Once the titanium is introduced, the Ti/HfO_2/Pt or the Pt/HfO_2/Ti/Pt RRAM device shows bipolar switching mode.[25] When positive bias is exerted on the Ti or the Ti intercalated electrode, the oxygen ions are driven towards and captured by Ti under the action of electric field and the high oxygen density of Ti. Oxygen vacancies accumulate in the HfO_2 layer, forming a conductive filament. When the applied bias is negative, the oxygen ions are released from Ti and annihilate the filament, finishing the RESET operation.

Figure 2(b) shows the typical electrical switching property of our Pt/HfO_2/Ti(5 nm)/Pt RRAM device. The electroforming occurs at −3.7-V bias. A compliance current (I_C) of 1 mA is applied during the following SET operations. A stable bipolar resistive switching is demonstrated (negative SET, positive RESET). The device in Fig. 2(b) experiences 65 switching cycles without degradation. The RESET voltages varies around +0.5 V, and the SET voltages spread in a range from −2.4 V to −1.5 V.

The above BRS mode bring the Pt/HfO_2/Ti(5 nm)/Pt into stable and robust switching behavior. But on the other hand, if we change the polarities of the BRS operation, *i.e.*, negative RESET and positive SET, the device is corrupted soon after only a few cycles. This phenomenon can be understood by the asymmetric structure of the device, which means that the drifting oxygen ions in HfO_2 can be stored only at the Ti intercalated electrode rather than the counter pure Pt electrode. Obviously, the polarity of the BRS operation in the device of Pt/HfO_2/Ti(5 nm)/Pt is unchangeable.

To implement the so-called any-polar resistive switching properties, the RRAM device needs to possess both the BRS and the URS properties simultaneously. Secondly, the polarities of both operations must be changeable. Finally, each operation mode and each polarity can be exchanged freely, which is independent of their operation history. Up to now, neither of the above two devices (Pt/HfO_2/Pt and Pt/HfO_2/Ti/Pt) can be called any-polar resistive switching device.

To implement the any-polar resistive switching mode, the key issue is the ability of the oxygen ions to be stored at both electrode sides of the resistive layer, considering that oxygen vacancy is the species to set up the filament. In the device of the Pt/HfO_2/Ti/Pt, oxygen ions can be stored only at the bottom electrode. So, adding another Ti intercalation layer to the top Pt electrode can straightforwardly improve the storage of oxygen. This idea leads to the symmetric device structure of Pt/Ti/HfO_2/Ti/Pt. A TEM cross-section image of the fabricated device is shown in Fig. 1(b).

For the symmetric Pt/Ti(5 nm)/HfO_2(10 nm)/Ti(5 nm)/Pt RRAM device, the resistive switching property is shown in Fig. 2(c). An electroforming process occurs at −3.725 V to

active the device. After forming, 120 uniform operation cycles are captured without any degradation. By recognizing the voltage polarity for each of the SET and the RESET process, all the switching operations can be grouped into four different resistive switching sub-modes, which are named as URS+, URS–, BRS+, and BRS– as shown in Fig. 2(d), respectively. In each conversion process, the conversion of two sub-switching modes is realized by changing the applied voltage polarity of one of the SET and the RESET process, with the voltage polarity of the other process remaining unchanged. In URS+, the SET and the RESET processes are both completed at positive voltages. For URS–, the SET and the RESET processes are both executed under negative voltages. For BRS+, the SET process is completed with negative bias, and the RESET process is completed with positive bias. For BRS–, opposite polarities of the SET and the RESET process may be determined by referring to the BRS+ mode.

The test in Fig. 2(c) starts from BRS+ mode. After 5–10 BRS+ cycles, the operation changes into the URS+ mode for another 5–10 cycles. The device subsequently undergoes the BRS– and URS– modes and finally comes back to the BRS+ mode. The above transition following the sequence of BRS+, URS+, BRS–, URS– is called a big-loop cycle. The device can also well follow the opposite big-loop cycle with the sequence of BRS+, URS–, BRS–, and URS+. Whether the mode is URS+ (or URS–) or BRS+ (or BRS–), the on-off ratio is always higher than 100, the absolute value of the SET and the RESET operation are both around 2.0 V and 0.5 V, respectively.

A comparison among the above three devices is shown in Fig. 3. The resistance distributions of both the HRS and the LRS at ±0.2 V for the three devices are shown in Fig. 3(a). Larger memory windows are observed for the Pt/HfO_2/Pt device without Ti intercalation than for the other two devices. But as already known, the Pt/HfO_2/Pt device suffers poor endurance. For the Pt/HfO_2/Ti/Pt device and the Pt/Ti/HfO_2/Ti/Pt device, both have stable distributions of the HRS and LRS resistances. The switching ratio of HRS to LRS for each device is generally larger than 100. A comparison of SET/RESET voltage distributions among the three devices is shown in Fig. 3(b). It is found that the SET/RESET voltage distributions of the bipolar Pt/HfO_2/Ti/Pt device fall well into those of the any-polar Pt/HfO_2/Ti/Pt device, which means that when the any-polar Pt/Ti/HfO_2/Ti/Pt device works in its BRS– sub-mode, its behavior is similar to that of the Pt/HfO_2/Ti/Pt device.

The migration of ions driven by electric field is the main motivation for resistive switching. Joule heating is another factor to redistribute ions. According to the type of the migration ions, electrochemical metallization memory and valance change memory are sorted. In the former, the conducting filaments are comprised of reduced active metal ions such as Ag+ or Cu+, which may drift, forming a metal electrode.[26–30] In the latter, the filaments are formed by oxygen vacancies.[6] The oxygen vacancy model is applicable for all the three devices in this work.

The Pt/HfO_2/Pt also has a symmetric device structure. Its URS property can also be observed with negative bias (denoted as URS–). The symmetric occurrence of URS+ and URS– is also called non-polar resistive switching mode.[9] However, further study finds that the conversion between the two URS modes is impossible. Frequently changing between the URS+ and the URS– causes the device to break down immediately.

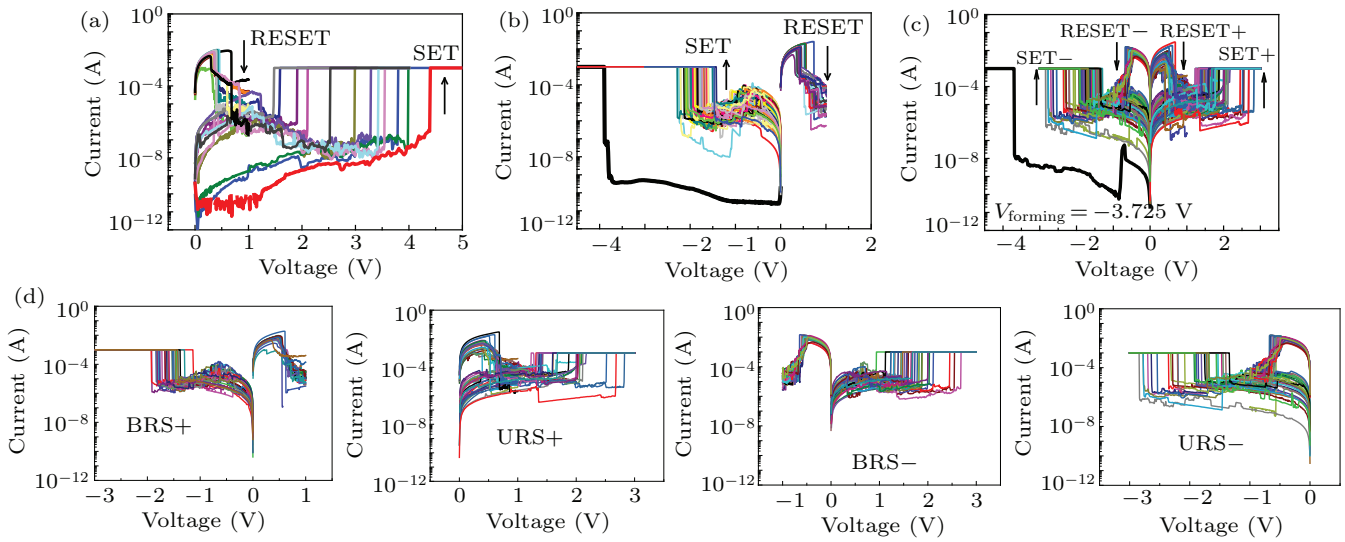

Fig. 2. Typical *I*–*V* switching characteristics based on HfO_2 RRAM with different Ti intercalation layers. (a) Unipolar resistive switching mode of Pt/HfO_2/Pt RRAM, (b) bipolar resistive switching mode of Pt/HfO_2/Ti(5 nm)/Pt RRAM, (c) any-polar resistive switching mode of Pt/Ti(5 nm)/HfO_2/Ti(5 nm)/Pt RRAM, and (d) four resistive switching sub-modes extracted from curves in panel (c).

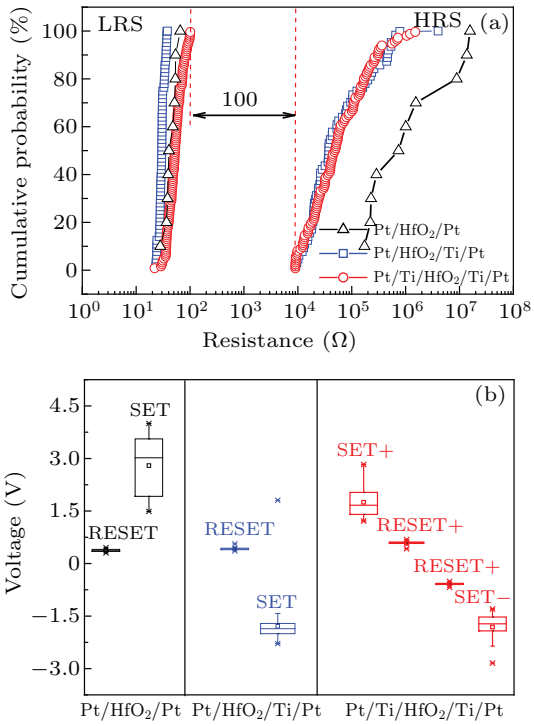

Fig. 3. (a) Switching resistance distributions of three devices of Pt/HfO_2/Pt, Pt/HfO_2/Ti/Pt and Pt/Ti/HfO_2/Ti/Pt at ±0.2 V. (b) SET and RESET voltage distributions of these devices.

The working mechanism of the bipolar Pt/HfO_2/Ti/Pt RRAM is depicted in Fig. 4(a). The restoring and releasing of oxygen ions by the Ti intercalation prevent oxygen ions from vanishing during the switching. Thus, the Pt/HfO_2/Ti/Pt device possesses a satisfactory endurance property. When adding Ti intercalation to both sides of the HfO_2 layer, both BRS+ and BRS– operations are now possible. The working mechanism of the Pt/Ti/HfO_2/Ti/Pt RRAM is depicted in Fig. 4(b).

When studying the RESET switches of the bipolar Pt/HfO_2/Ti/Pt device, Joule heating effect and the electric migration effect are difficult to clearly separate. Both are believed to contribute to the annihilation of the filaments. When considering the BRS+ and URS+ sub-modes in the any-polar device of Pt/Ti/HfO_2/Ti/Pt, it is comprehended that the migration effect may be helpful in implementing the operation of BRS+, but undoubtedly useless in the operation of UPS+. But in Fig. 2(d), the RESET curves of the BRS+ and URS+ sub-modes are nearly identical. Considering the similarity between the RESET curves of BRS+ and URS–, Joule heating effect rather than the migration effect should be the main mechanism during all the RESET switches for the Pt/Ti/HfO_2/Ti/Pt device, including all four sub-modes.

The any-polar resistive switching property was first proposed in the study of Pt/LATP/Pt.[18] The special switching property is ascribed to the unique crystalline structure of the LATP, which provides the abundant transport routes and storage sites for oxygen ions. In this study, the any-polar switching property is discovered in the Pt/Ti/HfO_2/Ti/Pt device. A comparison between both devices indicates that to fulfill the requirement for the any-polar resistive switching, the transport routes and the storage medium for oxygen ions do not have to be in the same layer. In the case of Pt/Ti/HfO_2/Ti/Pt, the HfO_2 acts as the transport route while the Ti intercalations serve as the storage medium. In this sense, if the HfO_2 layer is replaced by other conventional resistive oxides, such as Ta_2O_5[31] or TiO_2,[32] the any-polar resistance switching property can still be implemented.

Finally, the current transportation mechanisms of these types of devices are explored. Typical *I*–*V* curves of the Pt/HfO_2/Ti/Pt and Pt/Ti/HfO_2/Ti/Pt are re-plotted on a log–log scale as shown in Fig. 5. Whether they are in LRS or HRS, the Pt/HfO_2/Ti/Pt and Pt/Ti/HfO_2/Ti/Pt devices have the slopes of $\log(|I|)$ *versus* $\log(|V|)$ that are both close to unity, indicating that the ohmic conduction[33] is the dominant mechanism in LRS or HRS region.

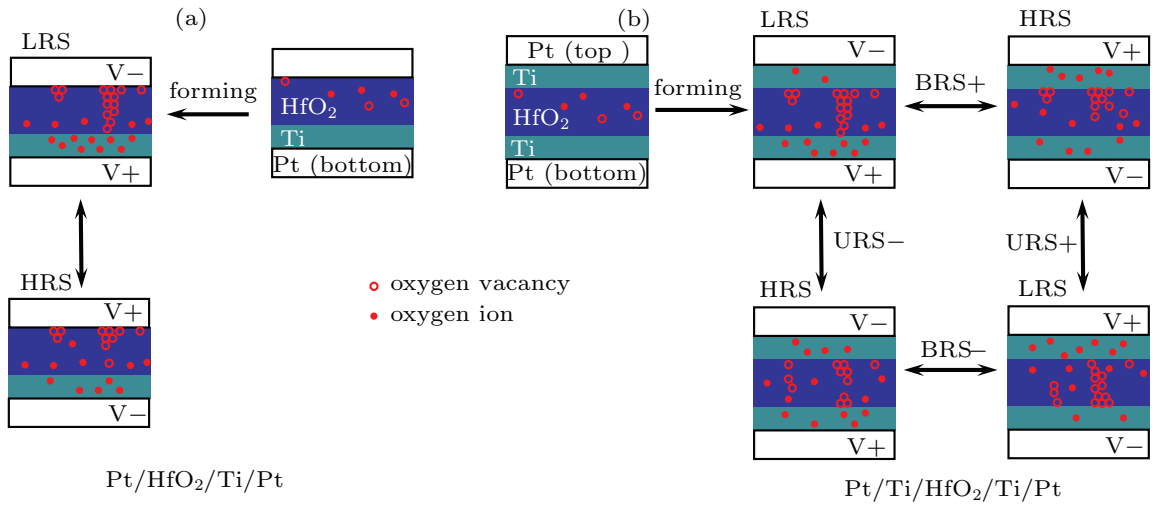

Fig. 4. Working mechanism of (a) Pt/HfO_2/Ti/Pt device and (b) Pt/Ti/HfO_2/Ti/Pt device. Notice that most of oxygen ions are stored in Ti intercalation layer. The four sub operation modes are URS+, URS–, BRS+, and BRS–.

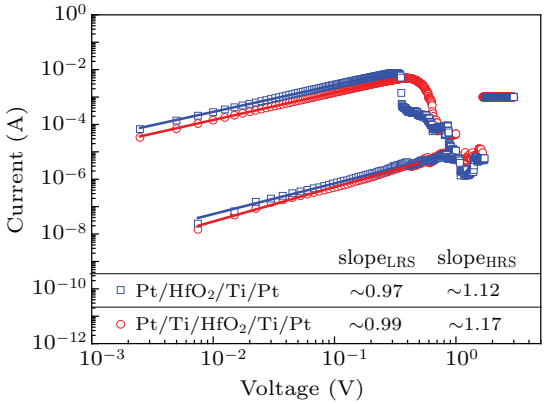

Fig. 5. Current fitting and current transportation mechanism of resistive switching properties, with blue and red lines representing Pt/HfO_2/Ti/Pt and Pt/Ti/HfO_2/Ti/Pt.

3. Conclusions

In summary, we demonstrate any-polar resistive switching behavior in Ti-intercalated Pt/Ti/HfO_2/Ti/Pt device. The any-polar resistive switching comprised of four sub-modes which are BRS+, URS+, BRS–, and URS–. The filaments formed by oxygen vacancies explain the switching mechanism. During switching, the HfO_2 acts as the transport route while the Ti intercalation layers serve as the storage medium. The investigation of the Pt/Ti/HfO_2/Ti/Pt RRAM presents a new insight into the fundamental working mechanism of the any-polar resistive switching device.

References

[1] Waser R and Aono M 2007 *Nat. Mater.* **6** 833
[2] Park I S, Kim K R, Lee S and Ahn J 2007 *Jpn. J. Appl. Phys.* **46** 2172
[3] Kang J and Park I S 2016 *IEEE Trans. Electron Dev.* **63** 2380
[4] Strukov D B and Likharev 2005 *Nanotechnology* **16** 888
[5] Rahaman S Z, Lin Y De, Lee H Y, Chen Y S, Chen P S, Chen W S and Wang P H 2017 *Langmuir* **33** 4654
[6] Lee S, Sohn J, Jiang Z, Chen H Y and Philip Wong H S 2015 *Nat. Commun.* **6** 8407
[7] Guan W, Long S, Liu Q, Liu M and Wang W 2008 *IEEE Electron Dev. Lett.* **29** 434
[8] F Pan, S Gao, C Chen, C Song and F Zeng 2014 *Mater. Sci. Eng. R* **83** 1
[9] Chen C, Gao S, Tang G, Song C, Zeng F and Pan F 2012 *IEEE Electron Dev. Lett.* **33** 1711
[10] Lin K L, Hou T H, Shieh J, Lin J H, Chou C T and Lee Y J 2011 *J. Appl. Phys.* **109** 084104
[11] Doo Seok Jeong, Schroeder H and Waser R 2007 *Electrochem. Solid-State Lett.* **10** G51
[12] Lee S, Kim H, Park J and Yong K 2011 *J. Appl. Phys.* **108** 076101
[13] Goux L, Lisoni J G, Jurczak M, Wouters D J, Courtade L and Muller C 2010 *J. Appl. Phys.* **107** 024512
[14] Xu D, Xiong Y, Tang M and Zeng B 2014 *J. Alloys Compd.* **584** 269
[15] Hao A, Ismail M, He S, Huang W, Qin N and Bao D 2018 *J. Appl. Phys.* **123** 085108
[16] Xu D L, Xiong Y, Tang M H, Zeng B W and Xiao Y G 2014 *Appl. Phys. Lett.* **104** 183501
[17] Hu W, Chen X M, Wu G H, Lin Y T, Qin N and Bao D H 2012 *Appl. Phys. Lett.* **101** 063501
[18] Jiao J L, Li L C, Cheng S, Chang A L, Mao Y C, Huang W and Chen S Y 2019 *Appl. Phys. Lett.* **115** 143506
[19] Key B, Schroeder D J, Ingram B J and Vaughey J T 2012 *Chemistry of Materials* **24** 287
[20] Aono H and Sugimoto E 1996 *J. Am. Ceram. Soc.* **79** 2786
[21] Aono H, Sugimoto E, Sadaoka Y, Aono H, Sugimoto E, Sadaoka Y, Imanaka N and Adachi G 1989 *J. Electrochem. Soc.* **136** 590
[22] González-Cordero G, Jiménez-Molinos F, Roldán J B, González M B and Campabadal F 2017 *J. Vac. Sci. Technol. B* **35** 01A110
[23] Lee H Y, Chen P S, Wu T Y, Chen Y S, Wang C C, Tzeng P J, Lin C H, Chen F, Lien C H, Tsai M J 2008 *IEEE International Electron Devices Meeting* (IEDM), 2008, December 15–17, San Francisco, CA, USA
[24] Jung Y C, Seong S, Lee T, Kim S Y, Park I S and Ahn J 2018 *Appl. Surf. Sci.* **435** 117
[25] Ge R, Wu X, Kim M, Shi J, Sonde S, Tao L and Akinwande D 2018 *Nano Lett.* **18** 434
[26] Cao M G, Chen Y S, Sun J R and Shen B G 2012 *Appl. Phys. Lett.* **101** 203502
[27] Singh N and Kaur D 2018 *Appl. Phys. Lett.* **113** 162103
[28] Tsuruoka T 2012 *Nanotechnology* **23** 435705
[29] Ge R, Wu X, Kim M, Shi J, Sonde S, Tao L and Akinwande D 2018 *Nano Lett.* **18** 434
[30] Kim H D, An H M, Hong S M and Kim T G 2012 *Semicond. Sci. Technol.* **27** 125020
[31] Lee M J 2011 *Nat. Mater.* **10** 625
[32] Acharyya D 2014 *Microelectronics Reliability* **54** 541
[33] Liu Q, Guan W H, Jiang P, Liu W F and Liu M 2008 *Appl. Phys. Lett.* **92** 012117